Acta Pharmaceutica Sinica B 2024;14(9):4174−4178

Chinese Pharmaceutical Association
Institute of Materia Medica, Chinese Academy of Medical Sciences

Acta Pharmaceutica Sinica B

www.elsevier.com/locate/apsb
www.sciencedirect.com

LETTER TO THE EDITOR

Allosteric regulation of Keap1 by 8β-hydroxy-α-cyclocostunolide for the treatment of acute lung injury

KEY WORDS

Macrophage overactivation;
Keap1;
8β-Hydroxy-α-cyclocostunolide;
Nrf2;
Acute lung injury

To the Editor:

Acute lung injury (ALI) is a debilitating lung disease characterized by pulmonary edema, diffuse alveolar damage, and uncontrolled neutrophil infiltration[1]. Severe cases of ALI can potentially lead to the development of acute respiratory distress syndrome (ARDS), which can lead to impaired respiratory function, multi-organ dysfunction, and an extremely high mortality rate[2-4]. ALI may be caused by various factors, including aspiration, severe pneumonia, sepsis, trauma, fatty embolism, pancreatitis, and blood transfusion[3]. Current clinical approaches to treating ALI/ARDS include mechanical ventilation, extracorporeal membrane oxygenation (ECMO), and other supportive therapies[5,6]. Therefore, ALI/ARDS is an urgent problem that needs to be addressed in the field of respiratory critical care and innovative mechanisms and therapies[6].

8β-Hydroxy-α-cyclocostunolide (HCC, Fig. 1A) is an eudesamane-type sesquiterpenoid that was first reported by Jakupovic in 1988[7]. Wu et al.[8] demonstrated that HCC inhibited the activation of macrophages, thereby reducing the release of lipopolysaccharide (LPS)-induced nitric oxide (NO) production, which highlights the potency of HCC in the treatment of inflammation. However, the mechanism and target of HCC in ALI remain to be fully understood. Herein, we synthesized a biotinylated probe by incorporating 8-aminocaproic acid and biotin into HCC. Through chemical genetics, we discovered that Keap1 was a direct target protein of HCC, which covalently bound to amino acid residues Cys257 and Cys288, leading to its conformational change and the blocking of kelch like ECH associated protein 1 (Keap1) with nuclear factor erythroid 2-related factor 2 (Nrf2). Furthermore, our findings revealed that chemical binding of Keap1 with HCC or Keap1 knockout (KO) suppressed macrophage overactivation in an LPS-induced ALI animal model. Taken together, these results demonstrated promising avenues for developing novel treatments for ALI by targeting Keap1, and suggested that HCC served as covalent modulators for Keap1.

1. HCC regulated IKKβ/IκBα/NF-κB and MAPKs pathways to block inflammation and redox imbalance *in vitro* and *in vivo*

First, we investigated cytotoxicity, anti-inflammatory, and antioxidant effects *in vitro* (Supporting Information Figs. S1−S3). HCC blocked the nuclear translocation of nuclear factor kappa B (NF-κB) p65 (Fig. S2F), dose-dependently suppressed releases of pro-inflammatory factors NO, interleukin (IL)-6, and tumor necrosis factor (TNF)-α, and downregulated expressions of inflammatory genes and proteins, such as TNF-α, inducible nitric oxide synthase (iNOS), monocyte chemotactic protein (MCP)-1, and cyclooxygenase (COX)-2, in LPS-challenged RAW264.7 cells (Fig. S2B−S2E). As illustrated in Supporting Information Fig. S3A−S3C, flow cytometry results HCC dose-dependently decreased the percentage of reactive oxygen species (ROS) positive cells. The redox imbalance was dose-dependently amended by HCC (Fig. S3D−S3F) *via* adjusting expressions of pro-oxidative and anti-oxidative genes [*e.g.*, NADPH oxidase (*NOX*)-2, catalase (*CAT*), and superoxide dismutase *1* (*SOD1*)] and proteins [*e.g.*, heme oxygenase (HO)-1, NAD(P)H dehydrogenase

Peer review under the responsibility of Chinese Pharmaceutical Association and Institute of Materia Medica, Chinese Academy of Medical Sciences.

https://doi.org/10.1016/j.apsb.2024.06.025

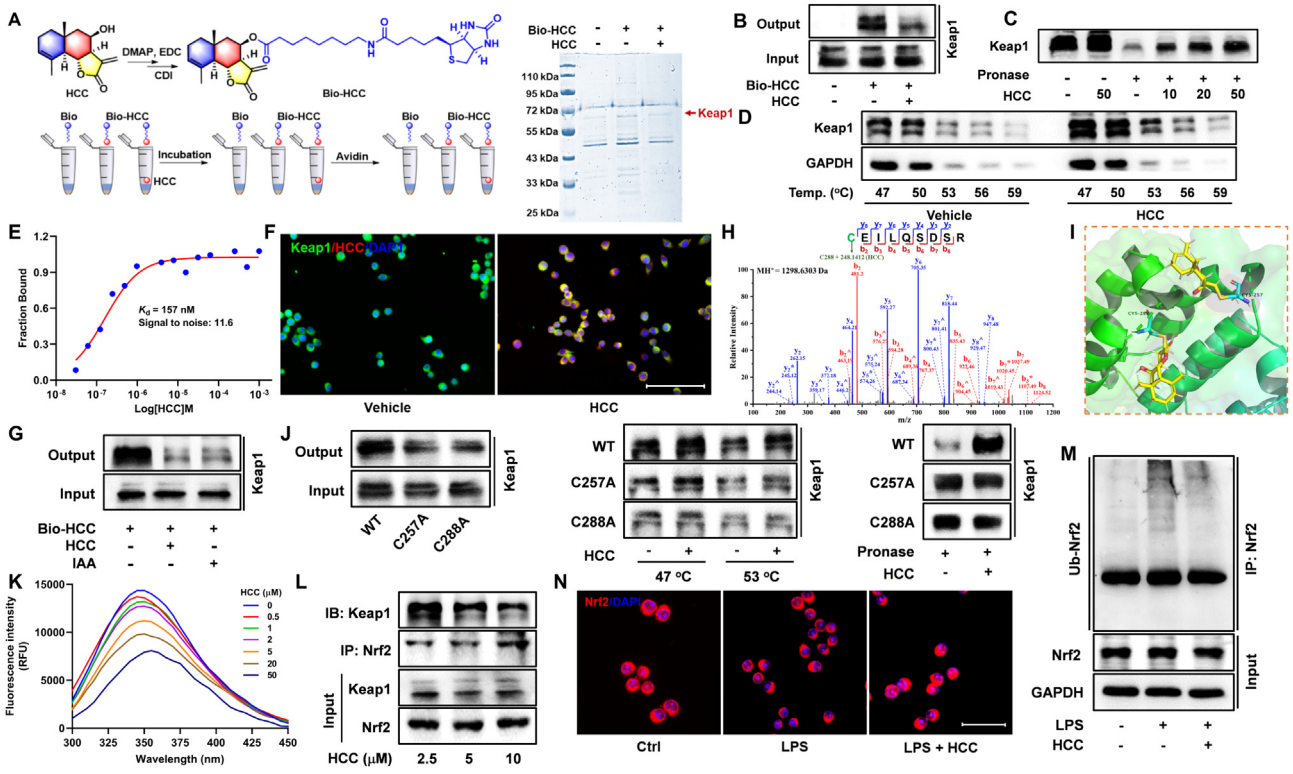

Figure 1 Keap1 served as a cellular direct target of HCC. (A) The synthesis of the biotinylated probe Bio-HCC and the schematic diagram of the biotin-streptavidin strategy and silver staining plot; (B) Pull down result detected by Western blot; (C) CETSA plot; (D) DARTS plot; (E) MST result of HCC and Keap1; (F) Immunofluorescence co-localization of HCC with Keap1; (G) IAA abolished the interaction of HCC with Keap1; (H) LC−MS/MS plot after the incubation of HCC with Keap1; (I) Molecular docking result; (J) Cys257Ala and Cys288Ala mutations weakened the binding of HCC with Keap1; (K) HCC led to the conformational change of Keap1 through the fluorescence titration experiment; (L) Co-IP result of Keap1 with Nrf2; (M) HCC inhibited Keap1-mediated Nrf2 ubiquitination; (N) HCC promoted the nuclear translocation of Nrf2.

(NQO)-1, and glutamate-cysteine ligase catalytic subunit (GCLC)]. We found that the decrease of LPS-induced mitochondrial membrane potential was reversed by HCC because JC-1 aggregate (red) was increased and JC-1 monomer (green) was decreased after HCC treatment (Fig. S3G). Notably, HCC blocked the increase of LPS-mediated mtDNA copy number and its release to cytoplasm according to the confocal experiment (Fig. S3H). Furthermore, HCC regulated the mitochondrial homeostasis *via* enhancing expressions of mitofusin-1 (Mfn1) and optic atrophy 1 (Opa1) and inhibiting the dynamin-1-like protein (Drp1) expression in a concentration-dependent manner (Fig. S3I and S3J).

The RNA-seq result suggested that the potential mechanism of HCC involved cytokine−cytokine receptor interaction, TNF, mitogen-activated protein kinases (MAPKs), and NF-κB pathways (Supporting Information Fig. S4A−S4C)[9,10], and HCC could regulate genes responsible for encoding inflammatory factors involved in cytokine−cytokine receptor interaction, such as *IL-1α*, *IL-1β*, *IL-6*, and C−C motif chemokine 5 (*CCL5*) (Fig. S4A−S4E). Our results revealed that HCC decreased mRNA levels of *IL-1α*, *IL-1β*, *IL-6*, and *CCL5* (Fig. S4F), and suppressed phosphorylations of inhibitor of nuclear factor kappa-B kinase subunit beta (IKKβ), NF-kappa-B inhibitor alpha (IκBα), and p65 involved in IKKβ-medicated NF-κB pathway and phosphorylations of ERK, JNK, and p38 involved in MAPKs pathway in RAW264.7 cells exposed by LPS (Figs. S4G and S5).

In an LPS-mediated ALI animal model, HCC treatment dose-dependently alleviated inflammatory cell infiltration, pulmonary edema, and collapse of alveolars, increasing of their wall thickness, and activation of macrophages induced by LPS treatment (Supporting Information Figs. S6 and S7A−S7C). Meanwhile, HCC ameliorated the increase of cytokines and pro-inflammatory genes (Supporting Information Figs. S7D, S7E, S8, S9A, and S9B) *in vivo*. Moreover, HCC ameliorated ROS-mediated mitochondrial imbalance *via* regulating IKKβ−NF-κB and MAPKs pathways in LPS-induced ALI mice (Supporting Information Figs. S9−S13). These data suggested anti-inflammatory and antioxidant effects of HCC through IKKβ−NF-κB and MAPKs pathways *in vitro* and *in vivo*.

2. Keap1 served as a direct cellular target of HCC

To uncover the cellular target of HCC, we synthesized a biotin labeling HCC probe (Bio-HCC, Fig. 1A) without significant influence toward its effects (Supporting Information Fig. S14). Its chemical structure was determined by NMR and HRMS spectra (Supporting Information Figs. S29−S37), requiring that the biotin side chain was linked at the hydroxy of C-8 for HCC. Subsequently, we conducted pull-down and silver staining experiments, which revealed the appearance of a prominent protein band at ~70 kDa (Fig. 1A). This protein was identified as Keap1 (Fig. S15) following in-gel digestion and LC−MS/MS experiments, which was further validated by Western blot using its specific antibody (Fig. 1B). The experimental results of drug affinity responsive target stability (DARTS) and cellular thermal shift

assay (CETSA) indicated that HCC stabilized Keap1 to resist influences of temperature and pronase on its stability (Fig. 1C and D, and Fig. S16), demonstrating the interaction of HCC and Keap1. Furthermore, the immunofluorescent co-localization analysis illustrated that HCC could directly bound to Keap1 (Fig. 1F). This finding was further supported by the microscale thermophoresis (MST) experiment, which showed a strong binding affinity between HCC and Keap1 with a K_d value of 157 nmol/L (Fig. 1E).

The si*Keap1* transfection caused the significant decrease of mRNA and protein expressions of Keap1, and its rescue led to the corresponding mRNA and protein overexpression as well (Fig. S17A, S17B, S17D, and S17E). Notably, *Keap1* knockdown led to the decrease of mRNA levels of *iNOS*, *COX-2*, *TNF-α*, *NOX-2*, and *MCP-1* and the increase of mRNA levels of *NQO-1*, *CAT*, and *SOD1* (Figs. S17C and S18) in LPS-induced cells, whereas protective effects of HCC toward inflammation and oxidative stress were significantly diminished in LPS-exposed *Keap1* knockdown cells (Figs. S17C and S18). To the contrary, *Keap1* overexpression led to the aggravation of LPS-mediated inflammation and oxidative stress (Fig. S17F), while distinctly impairing of anti-inflammatory and antioxidant effects of HCC after its rescue (Fig. S17F). These findings suggested the protective effect of HCC relied on Keap1.

3. HCC covalently bounded to Cys257 and Cys288 of Keap1 to block the interaction of Keap1 with Nrf2 depended on Nrf2

The pre-incubation of iodoacetamide (IAA) caused the decrease of Keap1 band intensity in Bio-HCC mediated pull-down experiment (Fig. 1G), which result was similar to the pre-incubation of HCC, suggesting the potential of HCC in covalent binding to Keap1. Next, we tried to perform the incubation experiment of HCC with recombinant human Keap1, and found that HCC covalently bound to Cys257 and Cys288 of Keap1 *via* analyzing the amino acid sequence of Keap1 using a LC−MS/MS system (Fig. 1H and Fig. S19A), which was further supported by molecular docking (Fig. 1I). Based on the pull-down experimental result, Cys257Ala (C257A) and Cys288Ala (C288A) mutations significantly impaired the binding of HCC with Keap1 (Fig. 1J), while reducing the pro-stability of HCC toward Keap1 in CETSA and DARTS experiments (Fig. 1J), which further supported by the MST experiment (K_d, 22.8 μmol/L for HCC with Keap1 C257A; K_d, 88.6 μmol/L for HCC with Keap1 C288A, Fig. S20). In addition, protective effects of HCC on inflammatory response and redox imbalance were abolished in LPS-mediated RAW264.7 cells after transfected Keap1 Cys257Ala and Cys288Ala (Fig. S19B).

Subsequently, we conducted a tryptophan fluorescence experiment, and HCC caused the decrease in the tryptophan fluorescence intensity of Keap1 (Fig. 1K), suggesting a substantial conformational change. Molecular dynamics stimulation (Figs. S21−S23) illustrated that HCC led to the conformational change of Gln337 and Pro384 in the binding cavity of Keap1 with ETGE motif (key moieties for their binding) of Nrf2, and the distance of Gln337 with Pro384 increased to 11.9 Å from 3.7 Å in the co−crystal of Keap1 with ETGE motif (PDB code 2FLU), which significantly caused the opening of the binding cavity of Keap1 with Nrf2 ETGE motif (Fig. S22B and S22C) to destroy interactions of Keap1 with ETGE motif (Fig. S23). This deduction was supported by Co-IP, ubiquitylation, and MST results (Fig. 1L, M, and Fig. S20C), therefore, HCC regulated the Nrf2 level *in vitro* and *in vivo* (Fig. S24A−S24C and Fig. 1N). Additionally, si*Nrf2* (Fig. S24D and S24E) caused the aggravation of LPS-challenged pro-inflammatory and pro-oxidant genes, including *TNF-α*, *iNOS*, *COX-2*, *MCP-1*, and *NOX-2*, while decreasing mRNA levels of *NQO-1* and *HO-1* in LPS-exposed RAW264.7 cells (Figs. S24F and S25). Notably, *Nrf2* knockdown weakened effects of HCC on inflammatory response and redox imbalance (Fig. S24F). These findings revealed that HCC blocked the interaction of Keap1 with Nrf2, and depended on Nrf2 to exert its anti-inflammatory and antioxidant effects.

4. Keap1 genetic knockout abolished the pulmonary protective effect of HCC *in vivo*

To determine whether protective effects of HCC against ALI *in vivo* was dependent on Keap1, *Keap1* KO mice were generated by deleting its exon 2. The genotype and Western blot results confirmed the successful *Keap1* genetic deletion (Fig. 2A−C). *Keap1* KO ameliorated LPS-mediated pulmonary structural changes (Fig. 2D−F), such as the inflammatory cell infiltration, pulmonary edema, and collapse of alveolars. This was attributed to the suppression of macrophage activation, which resulted in decreased levels of myeloperoxidase (MPO), TNF-α, IL-6, and malondialdehyde (MDA), while enhancing SOD and glutathione (GSH) levels in mice after LPS exposure (Fig. 2F, G, and Fig. S26). Furthermore, HCC treatment did not show additional effects in LPS-challenged ALI *Keap1*$^{+/-}$ mice (Fig. 2E−G and Fig. S26).

Finally, we explored protective effects of HCC on inflammatory response and redox imbalance in wild-type (WT, *Keap1*$^{+/+}$) and KO (*Keap1*$^{+/-}$) mice. Compared to LPS-induced ALI in WT mice, *Keap1* genetic deletion resulted in a significant decrease in COX-2 positive cells (Fig. S27A) and reduced mRNA levels of *IL-1α*, *IL-1β*, and *IL-6* (Fig. S27B). Furthermore, phosphorylations of key proteins p65, ERK, JNK, and p38 involved in NF-κB and MAPKs pathways were also suppressed (Figs. S27C, S27D, and S28). In addition, *Keap1* genetic deletion led to the increase of Nrf2 positive cells and mRNA levels of *SOD1* and *CAT* (Fig. S27E and S27F), while decreasing the *NOX-2* mRNA level (Fig. S27F) in mice challenged by LPS. Similarly, the Western blot analysis demonstrated that increasing of Nrf2 and HO-1 expressions is dependent on *Keap1* KO in LPS-challenged mice (Fig. S27G and S27H). However, HCC did not display additional effects in LPS-mediated ALI *Keap1*$^{+/-}$ mice (Figs. S27A−S27G and S28). In summary, these findings indicated the role of Keap1 in the treatment of HCC for ALI.

Collectively, we first reported that small molecule HCC covalently bound to Keap1 through the alkylation of Cys257 and Cys288, and disrupted its interaction with Nrf2 contributing to the inhibition of Nrf2 ubiquitylation and degradation. Furthermore, targeting Keap1 with HCC exerted anti-inflammatory and antioxidant effects *in vitro* and *in vivo*. In addition, the phenotype of ALI was attenuated in LPS-challenged mice after *Keap1* KO, and HCC did not significantly pulmonary protective effects in LPS-mediated *Keap1* KO mice. These results implied that targeting Keap1 to reduce inflammation and oxidative stress provided novel approaches for the treatment of ALI, and HCC could be a promising candidate for developing direct inhibitors of the Keap1−Nrf2 interaction.

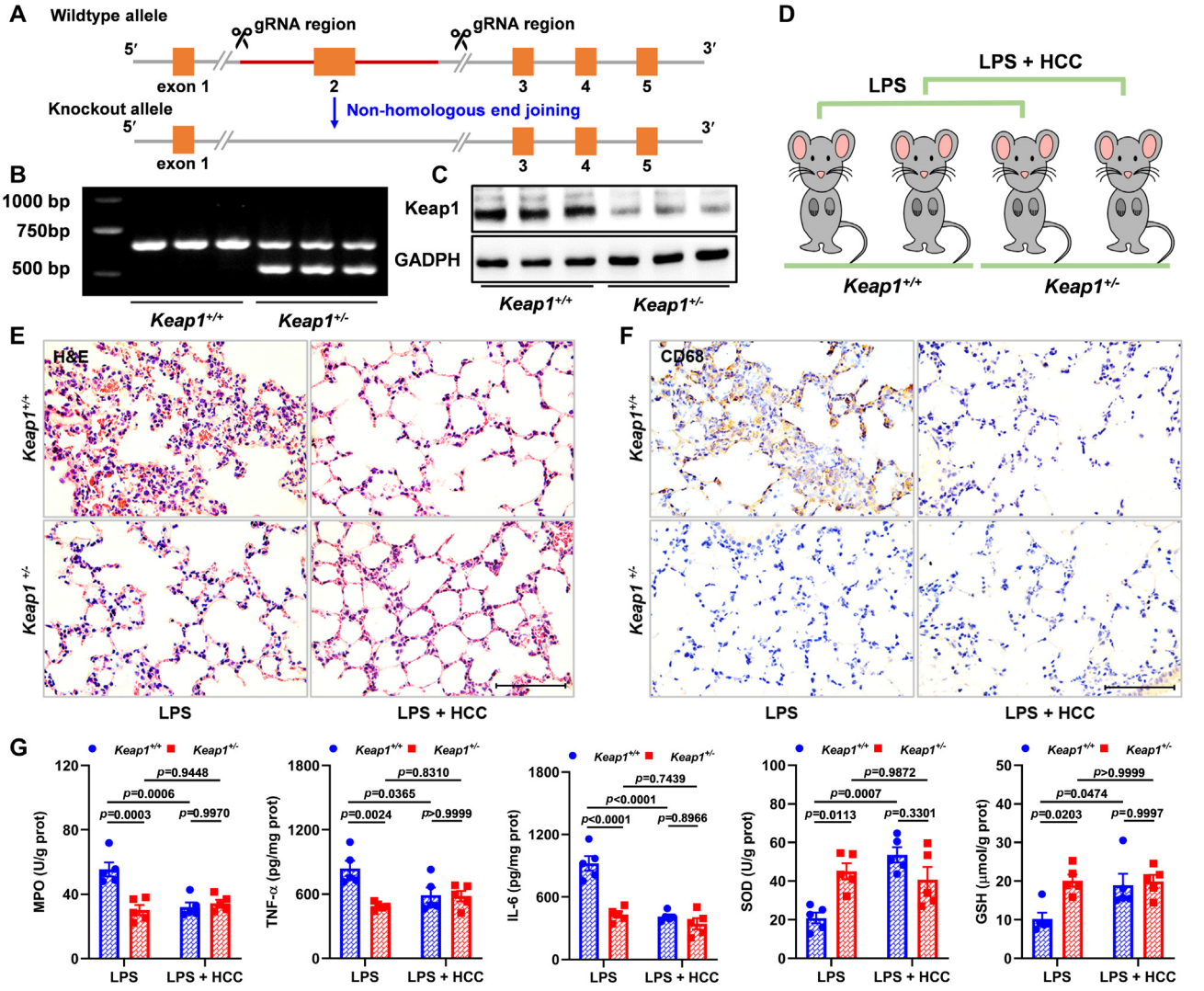

Figure 2 *Keap1* genetic KO abolished the pulmonary protective effects of HCC *in vivo*. (A) The construction of *Keap1* KO mice; (B, C) Genotyping and confirmation of *Keap1* KO mice; (D) Schematic diagram of LPS-mediated ALI in $Keap1^{+/+}$ and $Keap1^{+/-}$ mice; (E) Representative H&E plot; (F) Representative CD68 staining plot; (G) *Keap1* genetic KO abolished effects of HCC on MPO, TNF-α, IL-6, SOD, and GSH (mean ± SEM, $n = 5$).

Acknowledgments

This work is supported by National Natural Science Foundation of China (No. 82274069, 82030116, and 82141212), China Postdoctoral Science Foundation (No. 2022M720095 and 2023T160434), and Young Elite Scientists Sponsorship Program by China Association of Chinese Medicine (No. 2022-QNRC2-B09).

Author contributions

Juan Zhang: Writing − review & editing, Writing − original draft, Investigation, Funding acquisition. Min Zhang: Writing − original draft, Software, Investigation. Qi-Meng Zhu: Supervision, Project administration, Investigation. Xin-Rong Xu: Visualization, Supervision, Investigation. Yan-Li Feng: Project administration, Investigation. Sheng Lin: Writing − review & editing. Feng Qiu: Writing − review & editing, Funding acquisition. Cheng-Peng Sun: Writing − review & editing, Writing − original draft, Project administration, Investigation, Funding acquisition.

Conflicts of interest

The authors declare no competing interests.

Appendix A. Supporting information

Supporting information to this article can be found online at https://doi.org/10.1016/j.apsb.2024.06.025.

References

1. Xu D, Yang F, Chen J, Zhu T, Wang F, Xiao Y, et al. Novel STING-targeted PET radiotracer for alert and therapeutic evaluation of acute lung injury. *Acta Pharm Sin B* 2023;**13**:2124−37.
2. Derwall M, Martin L, Rossaint R. The acute respiratory distress syndrome: pathophysiology, current clinical practice, and emerging therapies. *Expert Rev Respir Med* 2018;**12**:1021−9.
3. Grommes J, Soehnlein O. Contribution of neutrophils to acute lung injury. *Mol Med* 2011;**17**:293−307.

4. Zhang J, Zhang M, Huo XK, Ning J, Yu ZL, Morisseau C, et al. Macrophage inactivation by small molecule wedelolactone *via* targeting sEH for the treatment of LPS-induced acute lung injury. *ACS Cent Sci* 2023;**9**:440−56.
5. Rios F, Iscar T, Cardinal-Fernandez P. What every intensivist should know about acute respiratory distress syndrome and diffuse alveolar damage. *Rev Bras Ter Intensiva* 2017;**29**:354−63.
6. Hopkins RO, Weaver LK, Collingridge D, Parkinson RB, Chan KJ, Orme JF Jr. Two-year cognitive, emotional, and quality-of-life outcomes in acute respiratory distress syndrome. *Am J Respir Crit Care Med* 2005;**171**:340−7.
7. Jakupovic J, Lehmann L, Bohlmann F, King RM, Robinson H. Sesquiterpene lactones and other constituents from *Cassinia, Actinobole* and *Anaxeton* species. *Phytochemistry* 1988;**27**:3831−9.
8. Wu RF, Zhou BD, Wang WQ, Chen T, Xu TT, Zhu SL, et al. Neolinulicin A and B from *Inula japonica* and their anti-inflammatory activities. *Fitoterapia* 2021;**152**:104905.
9. Zhang J, Luan ZL, Huo XK, Zhang M, Morisseau C, Sun CP, et al. Direct targeting of sEH with alisol B alleviated the apoptosis, inflammation, and oxidative stress in cisplatin-induced acute kidney injury. *Int J Biol Sci* 2023;**19**:294−310.
10. Sun CP, Zhou JJ, Yu ZL, Huo XK, Zhang J, Morisseau C, et al. Kurarinone alleviated Parkinson's disease *via* stabilization of epoxyeicosatrienoic acids in animal model. *Proc Natl Acad Sci U S A* 2022;**119**:e2118818119.

Juan Zhang[a,†], Min Zhang[a,†], Qi-Meng Zhu[a], Xin-Rong Xu[a], Yan-Li Feng[a], Sheng Lin[b,*], Feng Qiu[a,*], Cheng-Peng Sun[a,*]
[a]*School of Chinese Materia Medica, Tianjin Key Laboratory of Therapeutic Substance of Traditional Chinese Medicine, Tianjin University of Traditional Chinese Medicine, Tianjin 301617, China*
[b]*Key Laboratory of Chinese Internal Medicine of Ministry of Education and Beijing, Dongzhimen Hospital, Beijing University of Chinese Medicine, Beijing 100700, China*

*Corresponding authors.
E-mail addresses: lsznn@bucm.edu.cn (Sheng Lin), fengqiu20070118@163.com (Feng Qiu), suncp146@163.com (Cheng-Peng Sun).

[†]These authors made equal contributions to this work.

Received 9 April 2024
Received in revised form 8 June 2024
Accepted 20 June 2024